J. Phys.: Condens. Matter **10** (1998) 5069–5080. Printed in the UK PII: S0953-8984(98)88453-1

The instability of the cinnabar phase of ZnS under high pressure

A Qteish†, M Abu-Jafar‡ and A Nazzal§

† Department of Physics, Yarmouk University, Irbid-Jordan
‡ Department of Physics, An-Najah National University, Nablus, West-Bank
§ Department of Physics, Jordan University for Science and Technology, Irbid-Jordan

Received 15 October 1997, in final form 19 March 1998

Abstract. We present the results of a theoretical study of the structural phase transformations of ZnS under high pressure, using first-principles pseudopotential and full-potential linear muffin-tin orbital methods, in which the semicore Zn d electrons are treated as valence states. The zinc-blende, NaCl and cinnabar forms of ZnS have been considered. The structural properties and the band structures of these systems have also been studied. In the case of the FP-LMTO approach, an optimal choice of the empty spheres, atomic radii and filling percentage is introduced, which gives results in excellent agreement with those of the present pseudopotential method. It has been found that cinnabar phase is not a stable phase in ZnS under high pressure. The cinnabar phase is predicted to be a semiconductor with a direct band gap of about 3.6 eV.

1. Introduction

The structural phase transformations under high pressure in elemental and binary semiconductors have recently received a renewed interest. The results of the recent angle-dispersive x-ray measurements performed on many II–VI, III–V and group IV semiconductors under high pressures have altered significantly the widely accepted structural systematics [1]. New phases have been discovered, such as the cinnabar structure in CdTe [2], ZnTe [3] and GaAs [4], above the zinc-blende (ZB) phase, and the *Cmcm* form in several II–VI and III–V compounds; see reference [1]. The cinnabar phase in the above three systems is stable over a very narrow pressure range (about 2 GPa), and it is always observed on pressure decrease. It is worth noting that the cinnabar structure is the ground-state form of HgS, and was previously associated only with the Hg-based II–VI semiconductors. Therefore, the existence of this phase in other II–VI and III–V compounds is very interesting, and has prompted several theoretical investigations [5–8]. Côté *et al* [5] have studied the stability of the cinnabar and *Cmcm* phases in ZnSe, ZnTe, CdSe and CdTe, by using a first-principles pseudopotential plane-wave (PP-PW) method. They found that the observed cinnabar phase in ZnTe is realized by their calculations, but that this is not the case for CdTe. However, they have noted that the instability of the cinnabar structure in CdTe is very critical. Moreover, they have found a stable cinnabar phase in ZnSe, contrary to the experimental observations [9]. On the other hand, the stability of the cinnabar phase in CdTe is realized [6] by using a full-potential linear muffin-tin orbital (FP-LMTO) method [10]. Lee *et al* [7] have also confirmed by using a PP-PW method the stability of the cinnabar phase in ZnTe. Two of us [8] have studied the stability of the cinnabar phase in ZnS under high pressure, by using a PP-PW method, in which the semicore Zn 3d

0953-8984/98/235069+12$19.50

electrons are treated as a part of the frozen core and the non-linear exchange–correlation core corrections (NLCC) are included. According to these calculations the cinnabar form in ZnS is a stable high-pressure phase below the rock-salt (RS) structure. Therefore, extremely accurate theoretical calculations are required to study the stability of the cinnabar phase in the above semiconductors.

In this work we will reinvestigate the stability of the cinnabar phase in ZnS, by using a more advanced PP-PW method, which treats the Zn 3d electrons as valence states, and a FP-LMTO method (hereafter we will refer to the present PP-PW approach and that of reference [8] as the PP-PW and NLCC methods, respectively). In both approaches the local density approximation (LDA) was used for the exchange–correlation potential. The FP-LMTO method is an efficient and accurate approach for studying various properties of condensed matter systems. However, Muñoz and Kunc [11] have noted that the FP-LMTO results for the relative stability of different crystal structures of a certain material, and, hence, its high-pressure structural phase transformations, are sensitive to the computational ingredients (i.e., the choice of atomic radii of the true atoms and empty spheres (ESs), filling percentage (FP) and relativistic effects). The effects of these parameters on the above properties are thoroughly investigated, and an optimal choice for such parameters is introduced, which gives results in excellent agreement with those of the PP-PW approach. The crystal structures considered in this work are the ZB, RS and cinnabar structures. The electronic structures of these forms of ZnS have also been calculated, by using the FP-LMTO method.

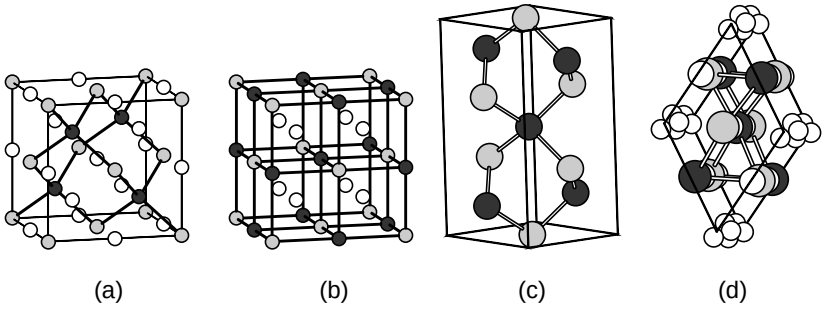

Figure 1. The unit cell of the ZB (a), RS (b) and cinnabar (c) crystal structures, and a view from almost directly above (along the c-direction) of the cinnabar unit cell (d). The empty spheres included are also shown as open circles, except for the cinnabar unit cell shown in (c). For the cinnabar phase we have used the calculated equilibrium values of v, u and the c/a ratio (see table 1), obtained by using the FP-LMTO approach.

2. Computational details

The unit cells of the ZB, RS and cinnabar structures are shown in figure 1, including the ESs considered. The β-Sn phase which has been ruled out as a high-pressure phase for ZnS [8] is not considered in this work. The ZB and RS structures can be fully described by just the lattice constant, a, whereas the cinnabar phase, which has a hexagonal unit cell of three ZnS formula units, has four structural parameters: a, the c/a ratio and two internal parameters, u and v for the Zn and S ions, respectively.

The ESs needed in the FP-LMTO calculations were chosen as follows. In the RS structure eight ESs were included in the conventional unit cell as shown in figure 1, giving

Table 1. Structural parameters of the zinc-blende, rock-salt and cinnabar phases of ZnS.

Structural parameter	Zinc-blende	Rock-salt	Cinnabar
a (Å)	5.352[a], 5.320[b], 5.280[c], 5.394[d], 5.580[e], 5.410[f]	5.017[a], 4.977[b], 4.943[c], 5.094[d], 5.210[e], 5.060[f]	3.765[a], 3.714[b], 3.671[c]
B_0 (GPa)	83.1[a], 83.4[b], 83.3[c], 82[d], 75.9[e],76.90[f]	104.4[a], 104.4[b], 107.62[c], 103.6[g]	89.3[a], 90.1[b], 91.2[c],
B_0'	4.43[a], 4.44[b], 3.92[c], 4.9[f]	4.28[a], 4.37[b], 4.10[c]	4.51[a], 4.53[b], 3.2[c]
c/a			2.256[a], 2.297[b], 2.336[c]
u			0.479[b], 0.488[c]
v			0.489[b], 0.495[c]

[a] Present work: relaxed d electrons, PP-PW calculations.
[b] Present work: FP-LMTO calculations.
[c] Reference [8]: PP-PW calculations, with NLCC.
[d] Reference [17]: LMTO calculations
[e] Reference [18]: Hartree–Fock calculations.
[f] Reference [19]: experimental data.
[g] Reference [17]: experimental data, obtained by using a fixed value of B_0' of 4.0.

four atoms (Zn, S and two ESs) per primitive unit cell. Similarly, eight ESs were included in the conventional unit cell of the ZB structure: three on the edges of the cube, one in its centre, and four as in the RS phase—at the vacant sites. For the cinnabar phase, with values of u and v of about 0.5, two sets of ESs (E1 and E2) each containing six ESs were included, per unit cell. The radius of an ES of type E2 is about 90% of that of the ES of the other type. The ESs of type E2 are located along the c-direction near the vertices of the unit cell in the perpendicular plane, while the ESs of type E1 lie at almost intermediate distances between the Zn and S atoms along the c-direction; see figure 1(d). The structural properties calculated using this method are quite insensitive to the inclusion of ESs, as already noted by Muñoz and Kunc [11]. This is not true for the calculated total energy, E_{tot}. Therefore, our search for the optimal values of these parameters at each of the considered volumes was conducted without the use of ESs. The ESs are, then, included in the optimized unit cell to calculate the E_{tot}-curves (E_{tot} versus V).

The radii of the Zn and S atoms and that of the ESs were chosen as follows. The radii of the Zn and S atoms were taken to be equal to each other and were assumed to be the same in the three crystal structures considered at the same value of V. For each of the values of V considered, they were considered to be equal to $0.97d/2$, where d is the bond length in the corresponding ZB structure. This gives, as a safety measure, an overlap of -3% between Zn and S atoms in the ZB structure, as proposed in reference [12]. This approach is different from the one adopted by Muñoz and Kunc [11], in which these radii (in the ZB and RS structures) are chosen to be equal at the volumes at which the phase transition occurs. This implies that the E_{tot}-curves of these two crystal structures are calculated with different FPs (larger in the case of RS). We believe that the present approach is more physical, and, as will be shown below, it leads to very good results, compared to those of the PP-PW approach. The effects of the FP on the transition pressure, p_t, of the ZB-to-RS

phase transformation in ZnS have been studied: using a value of the FP of 51.1, 53.9, 57.5 and 62.1%, the calculated value of p_t is of 13, 13.95, 15.3 and 17.28 GPa, respectively. The last FP value corresponds to equal radii for the atoms and the ESs and an overlap of -3% between them, in both the ZB and RS phases. This shows that the dependence of p_t on the FP is quite important, especially for delicate structural phase transformations, such as the present ones. Therefore, in our calculations, a fixed value of the FP is used for all volumes considered for the ZB, RS and cinnabar structures, which is determined by the values of the radii of ESs of the cinnabar form. In this phase and with the above choice for the radii of the Zn and S atoms, the radii of the allowed ESs are rather small: the zero overlap between these ESs gives a FP of 54.5%. In this work, we considered an average overlap between the ESs of about -1%, which gives a FP of 53.9%. At a value of V of 17 Å^3, the radii considered for the Zn, S, and the ESs of types E1 and E2, which satisfy the above requirements, are 1.0800, 1.0800, 0.8118 and 0.7326 Å, respectively. In going to other volumes, these values are simply scaled to maintain a fixed FP.

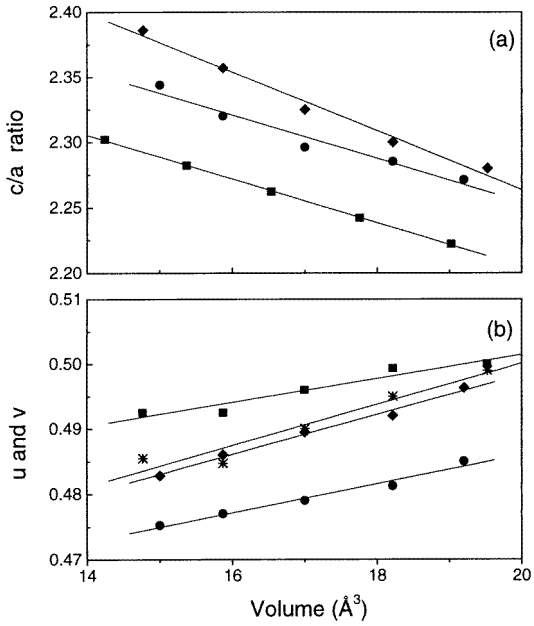

Figure 2. (a) The c/a ratios of the cinnabar phase of ZnS as a function of the volume per atom. Diamonds: the NLCC results. Circles: the FP-LMTO results. Squares: the data used in the PP-PW calculations; see the text. (b) As (a), but for the internal parameters (v and u). Squares and asterisks: the NLCC results for v and u, respectively. Diamonds and circles: the FP-LMTO results for v and u, respectively. The small dashed lines are the best linear fits to the calculated values.

The other computational details of the FP-LMTO calculations are as follows. We have used the Ceperley–Alder form of the LDA as parametrized by Vosko *et al* [13]. As the basis, we have used three Hankel functions per site with decay energies of -0.7, -1.0 and -2.3 Ryd. Each of the first two functions were expanded in terms of nine atomic orbitals, while only four atomic orbitals were used to expand the third one. This gives a total of twenty two basis functions per site. The Brillouin-zone integration was performed using 10 special $\boldsymbol{k}$-points for the ZB and RS structures and 34 special $\boldsymbol{k}$-points for the cinnabar

phase. The use of quite small sets of special $\boldsymbol{k}$-points is justified by the semiconducting behaviour of the three forms of ZnS considered. The scalar relativistic effects [14] are very important and, thus, have been included.

The computational details of the PP-PW calculations and the Zn and S pseudopotentials used are exactly as described in reference [8], for the relaxed d-electron calculations, and, therefore, will not be repeated here. In these calculations, the optimal c/a ratio and the internal parameters (u and v) of the cinnabar structure were determined by the constraint of isotropic stress and by minimizing the forces on the ions, respectively. This was done at only one value of a (3.7 Å). Then, the value of the c/a ratio obtained at this value of a together with the linear variation of the c/a ratio, as a function of V obtained by the FP-LMTO method (see figure 2), were used to find the c/a ratio for the other volumes considered. Moreover, the small variation of the values of u and v with respect to V was neglected. The effects of these assumptions were checked and they were found to alter the calculated E_{tot} by less than 5 meV/atom. Such energy differences are too small to affect our results and conclusions.

In the FP-LMTO approach, the optimal c/a ratio was obtained by calculating E_{tot} as a function of this parameter at a fixed value of V, and then fitting the resulting values to a parabola. Similarly, the u- and v-parameters were determined by minimizing E_{tot} at the calculated equilibrium c/a ratio. This was done without the use of ESs; see above. However, it turns out that E_{tot} is highly insensitive to the c/a ratio used (around the equilibrium values) at a fixed value of V. Therefore, the uncertainty in the determination of the structural parameters of the cinnabar structure, using this method, will not affect the calculated E_{tot}-curves. This has been checked by recalculating the E_{tot}-curves with the values of the c/a ratio used in the PP-PW calculations. The maximum difference in E_{tot} is found to be less than 2 meV/atom, whereas the difference in the value of the c/a ratio is 0.05 (see figure 2).

3. Results and discussion

3.1. Relative stability and structural parameters

The E_{tot}-curves of the ZB, RS and cinnabar phases of ZnS calculated by using the PP-PW and FP-LMTO approaches are shown in figure 3. These E_{tot}-curves were obtained by calculating E_{tot} at five different volumes, and fitting the calculated values to the Murnaghan equation of state. The two important features to note from figure 3 are as follows.

(i) First, the E_{tot}-curves for each of the above three structures calculated by using the PP-PW and FP-LMTO methods are very close to each other. The latter E_{tot}-curves are shifted almost rigidly by a very small amount to the left with respect to the former ones. The relative stabilities of both the cinnabar and RS structures with respect to the ZB form calculated by the above two methods are almost identical. The PP-PW and FP-LMTO results for the difference in the ground state E_{tot}, ΔE_{tot}, between the RS and ZB phases are 0.267 and 0.263 eV, respectively. In the case of the cinnabar structure, ΔE_{tot} takes the values 0.162 and 0.161 eV, respectively. This excellent agreement between the results of the PP-PW and FP-LMTO calculations demonstrates the soundness of our choice of the ESs and atomic radii, in the latter approach.

(ii) Second, the agreement between the results of the PP-PW and NLCC calculations of reference [8] is not satisfactory, especially in the case of the cinnabar structure: the NLCC results for ΔE_{tot} for the RS and cinnabar structures are 0.236 and 0.090 eV/atom, respectively. In the light of this large discrepancy between the NLCC results and that of

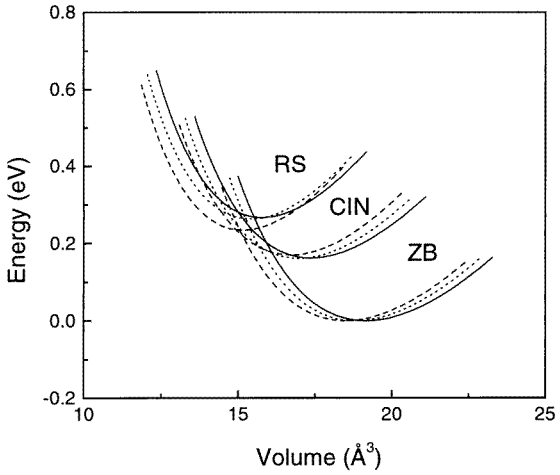

Figure 3. The total energy versus the volume per atom of the ZB, RS and cinnabar phases of ZnS. Solid curves: the PP-PW results. Dotted curves: the FP-LMTO results. Dashed curves: the NLCC results.

the above two approaches for the cinnabar phase, we have inspected our previous NLCC calculations. We have found that the calculations for the cinnabar phase were done using a slightly different S pseudopotential from the one used for the ZB and RS phases. After correcting this mistake, the NLCC results for the E_{tot}-curves (also shown in figure 3) are found to be in good agreement with the PP-PW and FP-LMTO results. The correct NLCC result for ΔE_{tot} for the cinnabar structures is 0.170 eV, which is also in very good agreement with the PP-PW and FP-LMTO results.

The calculated values of the structural parameters of the three forms of ZnS considered are listed in table 1, compared with the other available theoretical results and experimental data. The remarkable features to note from this table are as follows.

(i) The results of the PP-PW and FP-LMTO calculations for a_0, B_0 and B_0' for both the ZB and RS forms are in very good agreement with each other and with the available experimental data.

(ii) The NLCC results for these parameters are also in satisfactory agreement with experiment. It is worth noting here that our NLCC results are in better agreement with experiment than those of Engel and Needs [15]; for more details see reference [8].

(iii) The FP-LMTO results for the equilibrium volume per atom, V_0, for the three forms of ZnS studied are always slightly smaller than those of the PP-PW approach. The origin of such a discrepancy is not clear to us, but, fortunately, it has a very small effect on the calculated values of p_t; see below and figure 3.

(iv) The equilibrium values of u and v (about 0.5) for the cinnabar form of ZnS are similar to those observed for this phase in ZnTe and GaAs. For such values of u and v, the coordination number of the cinnabar phase is four, as for the ZB form. By considering the FP-LMTO results for the equilibrium structural parameters of the cinnabar phase (listed in table 1), we found that two of the four bonds around each of the Zn and S ions have a length of 2.326 Å, and the other two bonds a length of 2.356 Å. These values are slightly larger than the similarly calculated equilibrium. Moreover, the six equal bond angles in the ZB structure of 104.47° split in the cinnabar form of ZnS into two of 93.09°, two of

104.97°, one of 128.63° and one of 137.77°. Therefore, one can conclude that the local tetrahedral bonding structure in the cinnabar structure of ZnS is quite close to that of the ZB structure, which explains the presence of the E_{tot}-curve of this form between those of ZB and RS; see figure 3, and its electronic structure properties; see section 3.3.

(v) The values of B_0 for the cinnabar structure lie between those of the ZB and the RS forms. This feature, which was observed experimentally for HgTe (reference [16]), is consistent with the location of the equilibrium volume of this structure between those of the ZB and RS phases.

In figure 2, we show the variation of the optimal values of the c/a ratio, u and v for the cinnabar form, as functions of V, calculated by using the FP-LMTO and NLCC methods. The main features to note from this figure are as follows.

(i) The variations of both the FP-LMTO and NLCC results for the above three parameters, with respect to V, are almost linear.

(ii) The averaged difference between the values of both u and v calculated by the FP-LMTO and NLCC methods is very small (about 0.01).

(iii) The NLCC results for the c/a ratio are always larger than those obtained from the FP-LMTO calculations, on average by about 0.03. This difference increases to about 0.1 when the NLCC results are compared with the PP-PW ones (also shown in the same figure).

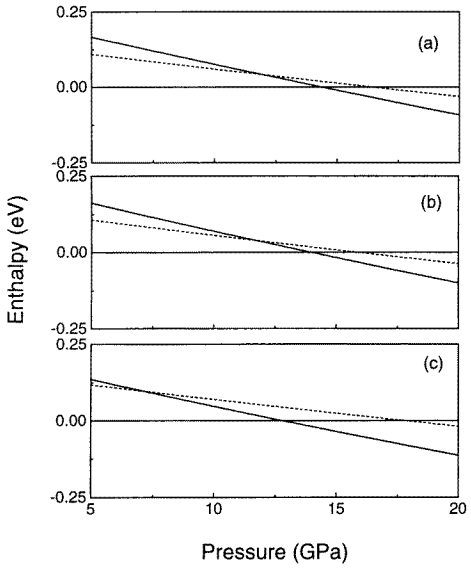

Figure 4. The static lattice enthalpy of the RS (solid lines) and cinnabar (dashed lines) forms of ZnS relative to that of the ZB phase, calculated via the PP-PW (a), FP-LMTO (b) and NLCC (c) approaches.

3.2. Phase transformations

The values of p_t for the ZB-to-RS and ZB-to-cinnabar structural phase transformations of ZnS under high pressure were determined from the constraint of equal static lattice enthalpy (per atom), given by

$$H(p) = E_{tot}(V(p)) + pV(p). \tag{1}$$

Table 2. The transition pressures (GPa) of ZnS, for the ZB-to-RS and ZB-to-cinnabar structural phase transformations. The other available theoretical and experimental data are also shown.

	Present work				
Phase transition	PP-PW (relaxed d electrons)	FP-LMTO	PP-PW (NLCC)	Other theoretical results	Experimental data
ZB to RS	14.35	13.95	12.99	16.1[a], 19.5[b]	14.7–15.4[c], 15.0–16.2[d], 18.1[e]
ZB to cinnabar	16.42	15.84	17.8		Not observed

[a] Reference [18]: Hartree–Fock calculations.
[b] Reference [17]: LMTO calculations.
[c] Reference [19].
[d] Reference [20].
[e] Reference [21].

The calculated $H(p)$ for the RS and cinnabar phases relative to that of the ZB phase are shown in figure 4. The values of p_t obtained by using the above three theoretical approaches are shown in table 2, compared with the other available theoretical results and experimental data. The remarkable features to note from these results are as follows.

(i) The excellent agreement between the our results, obtained by using the three approaches considered, especially between the FP-LMTO and the PP-PW results.

(ii) For the ZB-to-RS phase transition, the values of p_t calculated by using the FP-LMTO and the PP-PW approaches (14.35 and 13.95 GPa, respectively) are also in excellent agreement with the experimental value (about 15 GPa). The NLCC result (12.8 GPa) is in reasonable agreement with experiment.

(iii) The results of these three theoretical approaches show that the cinnabar phase is not a stable high-pressure phase in ZnS. The values of p_t for the ZB-to-cinnabar phase transition are 2.07, 1.89 and 5 GPa higher than those of the ZB-to-RS phase transition, respectively, in the case of the PP-PW, FP-LMTO and NLCC calculations.

The volume contractions associated with the ZB-to-RS phase transition, defined as $\Delta V/V_t(\mathrm{ZB})$, calculated by using the PP-PW, FP-LMTO and NLCC approaches are 0.160, 0.153 and 0.160, respectively. Here, $V_t(\mathrm{ZB})$ is the volume of the ZB structure at which the above transition occurs. These results are in very good agreement with the experimental value of 0.157 (reference [17]).

3.3. Electronic structure

The band structure of the ZB phase of ZnS calculated by using the FP-LMTO technique is shown in figure 5. The corresponding eigenvalues at the high-symmetry points in the Brillouin zone for this structure are listed in table 3, compared with the other calculated values and the available experimental data. The two features to note from these results are as follows.

(i) It is evident that the eigenvalues calculated by using the FP-LMTO method are in excellent agreement with those obtained using the PP-PW method. The maximum difference is in the position of the d bands, of 0.18 eV. For this reason, we have calculated the band structures of the three phases of ZnS considered by using just the FP-LMTO technique.

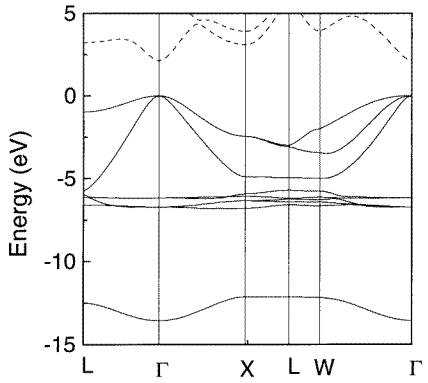

Figure 5. The band structures of the ZB structure of ZnS calculated at the experimental lattice constant, by using the FP-LMTO method. The conduction and valence bands are shown by dashed and solid lines, respectively.

Table 3. The FP-LMTO results for the energy levels (eV) at high-symmetry $\boldsymbol{k}$-points of the zinc-blende form of ZnS, compared with results of the PP-PW (references [22] and [23]) and linearized augmented-plane-wave (LAPW) (reference [23]) methods, and the available experimental data.

Eigenvalues	FP-LMTO	PP-PW, reference [22]	PP-PW, reference [23]	LAPW, reference [23]	Experiment, reference [19]
Γ_{1v}	−13.12	−13.21	−13.07	−13.11	−13.50
Γ_{15v} (d)	−6.47	−6.65	−6.63	−6.55	∼−10.00
Γ_{12v} (d)	−5.99	−6.17	−6.16	−6.09	∼−10.00
Γ_{15v}	0.00	0.00	0.00	0.00	0.00
Γ_{1c}	1.84	1.79	1.84	1.81	3.80
Γ_{15c}	6.27	6.21	6.15	6.19	8.35
X_1	−11.86	−11.92	−11.77	−11.84	−12.00
X_{3v}	−4.66	−4.77	−4.74	−4.70	−5.50
X_{5v}	−2.23	−2.32	−2.29	−2.25	−2.50
X_{1c}	3.22	3.19	3.19	3.18	
X_{3c}	3.91	3.90	3.87	3.87	4.90
L_1	−12.18	−12.24	−12.10	−12.16	−12.40
L_{1v}	−5.36	−5.47	−5.43	−5.38	−5.50
L_{3v}	−0.87	−0.92	−0.90	−0.88	−1.4
L_{1c}	3.10	3.30	3.05	3.05	
L_{3c}	6.85	6.78	6.75	6.76	

(ii) The LDA band gap of this system is 1.84 eV, which is 48.4% of the experimental value (3.8 eV). The LDA underestimation of the energy band gaps of semiconductors is well known, and can be largely removed by using sophisticated many-body methods, such as the GW technique [24].

The band structure of the cinnabar form of ZnS is shown in figure 6. This system is found to be a direct-band-gap semiconductor, with an LDA band gap at the Γ point of 1.64 eV, which is very close to that of the ZB form. Moreover, the widths of the d and valence bands of the cinnabar phase of ZnS are larger than those of the corresponding bands of the ZB form by only 0.3 to 0.4 eV, respectively. This behaviour is not surprising, since

in the cinnabar structure with values of u and v of about 0.5 the distortions from the local tetrahedral bonding are quite small; see section 3.1. To get an idea of the fundamental band gap of the cinnabar form of ZnS, we have assumed that the many-body effects are wavevector independent, and they are the same in the ZB and cinnabar structures of ZnS. Therefore, we have used the so-called scissors operator to rigidly shift the conduction bands up in energy by 1.96 eV, to recover the experimental band gap of the ZB form, giving a value for the fundamental band gap of the cinnabar phase of 3.6 eV. The use of the same scissors operator for these two forms of ZnS is justified by the above close similarity in their band structures. It is worth mentioning that similar electronic structure modifications are expected in the case of GaAs and ZnTe, on going from ZB to cinnabar phases, since their equilibrium values of u and v are about 0.5.

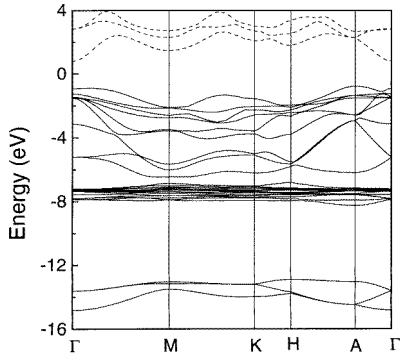

Figure 6. As figure 5, but for the cinnabar phase at the calculated equilibrium geometry.

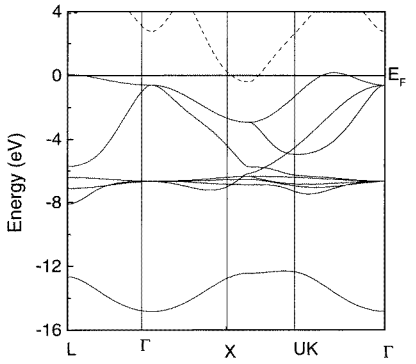

Figure 7. As figure 5, but for the RS form at the onset of the ZB-to-RS phase transition, with a_0 equal to 4.872 Å. This value of a_0 is obtained by subtracting from the volume of the ZB structure at which the above transition occurs the associated value of the volume contraction. We used the experimental data reported in table I of reference [17]. E_F refers to the Fermi energy.

The calculated band structure of the RS phase of ZnS, at the onset of the ZB-to-RS phase transition, is shown in figure 7, which shows that it has a small negative LDA band gap. However, the above many-body effects will shift the conduction bands up in energy with respect to the valence ones. This makes the RS phase of ZnS an indirect-band-gap semiconductor, with two valence band maxima along the Σ direction and at the L point,

and a conduction band minimum at the X point. The maximum along the Σ direction is slightly higher in energy than the one at the L point (by about 0.1 eV). These results are in excellent agreement with the LMTO calculations and the experimental results, which show that this system is a semiconductor with an indirect band gap of about 2.0 eV, as reported in reference [17].

4. Conclusions

The stability of the cinnabar phase in ZnS under high pressure is reinvestigated by using the first-principles pseudopotential plane-wave (PP-PW) and full-potential linear muffin-tin orbital (FP-LMTO) techniques, in which the Zn 3d electrons are treated as valence states. We have also repeated the PP-PW calculations of reference [8], in which the Zn 3d electrons are treated as a part of the frozen core and the non-linear exchange–correlation core corrections (NLCC) are included. Moreover, the band structure of the three crystal structures considered (zinc-blende (ZB), rock-salt (RS) and cinnabar) are calculated via the FP-LMTO method. In the following, we draw our main results and conclusions.

(i) In the case of the FP-LMTO method, we have introduced an optimal choice for the empty spheres and atomic radii, which gives results in excellent agreement with those obtained by using the PP-PW approach.

(ii) Although the cinnabar form of ZnS is found to be more stable than the RS form, it has been excluded from consideration as a high-pressure phase in ZnS.

(iii) The previous NLCC results for the stability of the cinnabar phase are incorrect, and this approach gives results in good agreement with the above two methods, for both the relative stability and the structural parameters of the phases of ZnS considered.

(iv) The cinnabar phase of ZnS is a semiconductor with a direct band gap at the Γ point of about 3.6 eV.

(v) At the onset of the ZB-to-RS phase transition, the RS form of ZnS is also a semiconductor with an indirect band gap, with two valence band maxima along the Σ direction and at the L point, and a conduction band minimum at the X point.

Acknowledgments

Part of this work was done at the International Centre for Theoretical Physics (ICTP), Trieste, Italy. One of us (AQ) would like to acknowledge the Associateship Scheme of the ICTP for financial support. One of us (MA) would like to acknowledge the ICTP and the Centre for Theoretical and Applied Physics at Yarmouk University, Irbid-Jordan, for financial support and kind hospitality. We are indebted to Michael Methfessel for providing us with his FP-LMTO code. Many thanks go to Rubin Weht for his kind help with the FP-LMTO code and for interesting discussions. We are grateful to Karel Kunc, Mark van Schilfgaarde, Malcolm McMahon and Richard Nelmes for stimulating discussions.

Note added in proof. After we finished this work, we were informed by R Nelmes and M McMahon that they have studied the high-pressure structural phase transformations of ZnS under high pressure and that they have not observed a cinnabar phase in this compound, in agreement with the results of the present work.

References

[1] For a recent review, see

McMahon M I and Nelmes R J 1996 *Phys. Status Solidi* b **198** 389
[2] McMahon M I, Nelmes R J, Wright N G and Allan D R 1993 *Phys. Rev.* B **48** 16 246
[3] McMahon M I, Nelmes R J, Wright N G and Allan D R 1994 *Phys. Rev. Lett.* **73** 1805
[4] McMahon M I and Nelmes R J 1997 *Phys. Rev. Lett.* **78** 3697
[5] Côté M, Zakharov O, Rubio A and Cohen M L 1997 *Phys. Rev.* B **55** 13 025
[6] Ahuja R, James P, Eriksson O, Wills J M and Johansson B 1997 *Phys. Status Solidi* b **199** 75
[7] Lee G-D and Ihm J 1996 *Phys. Rev.* B **53** R7622
Lee G-D, Hwang C, Lee M H and Ihm J 1997 *J. Phys.: Condens. Matter* **9** 6619
[8] Nazzal A and Qteish A 1996 *Phys. Rev.* B **53** 8262
[9] McMahon M I 1997 private communications
[10] Methfessel M, Rodriguez C O and Andersen O K 1989 *Phys. Rev.* B **40** 2009
[11] Muñoz A and Kunc K 1994 *Comput. Mater. Sci.* **2** 400
[12] Fiorentini V, Methfessel M and Scheffier M 1993 *Phys. Rev.* B **47** 13 353
[13] Vosko S H, Wilk L and Nusair M 1980 *Can J. Phys.* **58** 1200
Wilk L and Vosko S H 1982 *J. Phys. C: Solid State Phys.* **15** 2139
[14] Methfessel M 1988 *Phys. Rev.* B **38** 1537
[15] Engel G E and Needs R J 1990 *Phys. Rev.* B **41** 7876
[16] San-Miguel A, Wright N G, McMahon M I and Nelmes R J 1995 *Phys. Rev.* B **51** 8731
[17] Ves S, Schwarz U, Christensen N E, Syassen K and Cardona M 1990 *Phys. Rev.* B **42** 9113
[18] Jaffe J E, Pandey R and Seal M J 1993 *Phys. Rev.* B **47** 6299
[19] *Numerical Data and Functional Relationships in Science and Technology; Landolt–Börnstein New Series* 1982 Group III, vol 17b, ed O Madelung *et al* (Berlin: Springer)
[20] Piermarini G J and Block S 1975 *Rev. Sci. Instrum.* **46** 973
Yu S C, Spain I L and Skelton E F 1978 *Solid State Commun.* **25** 49
Yagi T and Akimoto S 1976 *J. Appl. Phys.* **47** 3350
Onodera A and Ohtani A 1980 *J. Appl. Phys.* **51** 2581
[21] Samara G A and Drickamer H G 1962 *J. Phys. Chem. Solids* **23** 457
[22] Qteish A, Said R, Meskini N and Nazzal A 1995 *Phys. Rev.* B **52** 1830
[23] Martins J L, Troullier N and Wei S-H 1991 *Phys. Rev.* B **43** 2213
[24] See, for example,
Godby R W, Schlüter M and Sham L J 1987 *Phys. Rev.* B **36** 6497 and references therein